European Journal of Medicinal Chemistry 57 (2012) 373–382

Contents lists available at SciVerse ScienceDirect

European Journal of Medicinal Chemistry

journal homepage: http://www.elsevier.com/locate/ejmech

Original article

Design, synthesis and antibacterial activities of vanillic acylhydrazone derivatives as potential β-ketoacyl-acyl carrier protein synthase III (FabH) inhibitors

Xiao-Liang Wang, Yan-Bin Zhang, Jian-Feng Tang, Yu-Shun Yang, Ruo-Qi Chen, Fei Zhang, Hai-Liang Zhu*

State Key Laboratory of Pharmaceutical Biotechnology, Nanjing University, Nanjing, 210093, PR China

ARTICLE INFO

Article history:
Received 10 July 2012
Received in revised form
24 August 2012
Accepted 6 September 2012
Available online 13 September 2012

Keywords:
FabH inhibitor
Antibacterial
Hemolytic activity
Acylhydrazone

ABSTRACT

Fatty acid biosynthesis is essential for bacterial survival. FabH, β-ketoacyl-acyl carrier protein (ACP) synthase III, is a particularly attractive target, since it is central to the initiation of fatty acid biosynthesis and is highly conserved among Gram-positive and Gram-negative bacteria. A series of acylhydrazone derivatives were synthesized and developed as potent inhibitors of FabH. This inhibitor class demonstrates strong broad-spectrum antibacterial activity. Compounds with potent antibacterial activities were tested for their *Escherichia coli* FabH inhibitory activity. Especially, compound **E9** showed the most potent antibacterial activity with MIC values of 0.39–1.56 μg/mL against the tested bacterial strains and exhibited the most potent *E. coli* FabH inhibitory activity with IC_{50} of 2.5 μM. Docking simulation was performed to position compound **E9** into the *E. coli* FabH active site to determine the probable binding conformation.

1. Introduction

Bacterial infection remains a serious threat to human lives because of emerging resistance to existing antibiotics, which is an increasing public health problem [1]. In order to prevent this serious medical problem, the elaboration of new types of antibacterial agents or the expansion of bioactivity of the previous drugs is a very important task [2]. To meet critical clinical needs, especially to overcome the emerging drug resistance, the discovery of novel antibiotic chemical scaffolds with new modes of action is crucial for saving lives. Fatty acid biosynthesis (FAB) is an essential metabolic process for prokaryotic organisms and is required for cell viability and growth [3]. Significant differences between bacterial and human fatty acid synthesis systems exist that include the organization and structure of enzymes and the specific roles played by fatty acids make this system an attractive target for antibacterial drug discovery [4,5]. The β-ketoacyl-acyl carrier protein synthase III (FabH) is one of essential functional enzymes in FAS II, which initiates the FAB cycle by catalyzing the first condensation step between acetyl-CoA and malonyl-ACP, playing a key regulatory role in the bacterial FAB cycle (Fig. 1) [6]. Additionally, FabH is highly conserved among key pathogens while there are no significantly homologous proteins in humans [7]. Importantly, the residues that comprise the active site are essentially invariant in various bacterial FabH molecules [8,9]. These attributes suggest that small molecule inhibitors of FabH enzymatic activity could be potential development candidates leading to selective, nontoxic and broad-spectrum antibacterial agents.

Thus, various kinds of compounds were screened by enzymatic assays and subsequently optimized using structure guided drug design methods [7,10–19]. Compounds containing Schiff base moiety or hydrozone moiety show antimicrobial activity against various bacteria, including inhibitors of FabH, which were reported in the previous studies of our laboratory [13–17] and Kim et al. [18,19]. For example, compounds (**11** and **18** [13]; **19** [14]; **10** [15]; **2d** [16]; **12** and **13** [17]; **YKAs3003** [18]; **6**, **6c** and **6e** [19]) reported as inhibitors of *Escherichia coli* FabH showed the most potent antibacterial activity and FabH inhibitory activity in each article respectively, which are displayed in Fig. 2. As shown in Fig. 2, these compounds share similar core structures. Obviously, there always exists a benzene-1,3-diol or benzene-1-ol group and a hydrazone moiety (–NH–N=CH–) or a Schiff base moiety (–C=N–) in the core structures. Taking into account the instability of hydrazone moiety and Schiff base moiety, the N-acylhydrazone moiety (–CO–NH–N=CH–) was considered as a privileged structure employed to improve the chemical stability for the design of new FabH inhibitors. Moreover, acylhydrazones have aroused considerable attention due to their particular physical, chemical, and biological activities based on their unique structures and they are known to present a wide spectrum of biological properties, such as antimicrobial activity against several bacteria [20,21].

* Corresponding author. Tel.: +86 25 8359 2572; fax: +86 25 8359 2672.
E-mail address: zhuhl@nju.edu.cn (H.-L. Zhu).

0223-5234/$ – see front matter © 2012 Elsevier Masson SAS. All rights reserved.
http://dx.doi.org/10.1016/j.ejmech.2012.09.009

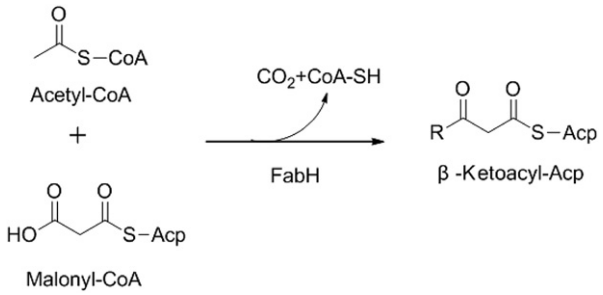

Fig. 1. FabH accomplishes the initial condensation step in FAS II.

Compounds containing a benzene-1-methoxy-2-ol scaffold also have received significant attention in natural medicinal chemistry research as this structural scaffold is found in a variety of natural products. As shown in Fig. 3, vanillic acid (**A**), which is found in many traditional Chinese medicines, such as *Rhizoma Picrorhizae*, *Ginseng*, *Propolis* and *BaiHao*, has been reported to possess antimicrobial activity [22]. Ferulic acid (**B**) is also an active ingredient of many Chinese herbal medicines, such as *Chuanxiong*, *Danggui* and *Awei*, which have been used to treat cardiovascular diseases by Chinese physicians for thousands of years [23]. Curcumin (**C**), the active ingredient in the traditional herbal remedy *turmeric*, has a surprisingly wide range of beneficial properties, including antioxidant [24], anti-inflammatory [25,26], antimicrobial [27] and anti-cancer [28] activity, so curcumin research has been a hot scientific topic of study. Eugenol (**D**) exhibits an excellent broad-spectrum bactericidal activity [29]. Silymarin (**E**) is well known as a kind of hepatoprotective herbal drug [30]. Hesperidin (**F**) is clinically taken supplements along with vitamin C to treat diseases like purpura and scurvy as hesperidin can promote vitamin C more easily absorbed because of its beneficial effects on the blood vessels.

In view of the above mentioned findings, we report in the present work the synthesis of a series of acylhydrazone derivatives to extend the research to achieve new potential antibacterial FabH inhibitors by structural optimization. The benzene-1-methoxy-2-ol moiety was introduced to enhance the molecular interactions, which based on the results of CADD (computer assistant drug design). With the benzene-1-methoxy-2-ol moiety fixed, we introduced different substituents on the other benzene ring which connected with the azomethine moiety (−C═N−) to study the structure−activity relationships in antibacterial activity for further optimization. Thus we studied their antimicrobial activities and *E. coli* FabH inhibitory activities. Docking simulations were performed using the X-ray crystallographic structure of the FabH of *E. coli* in complex with the most potent inhibitor to explore the binding model of the compound at the active site.

2. Results and discussion

2.1. Chemistry

In this study, 30 vanillic acylhydrazone derivatives (**E1**−**E30**) were synthesized. The synthetic route of compounds **E1**−**E30** was shown in Scheme 1. They were synthesized from 4-hydroxy-3-methoxybenzoic acid (**A**). Esterification of the 4-hydroxy-3-methoxybenzoic acid with methanol and concentrated sulfuric acid afforded the corresponding ester **B**. The aroyl hydrazide **C** was obtained by reacting **B** with 85% hydrazine monohydrate in ethanol. The synthesis of compounds **E1**−**E30** was accomplished by reacting **C** with aldehyde **D** in ethanol [31].

All of the synthetic compounds gave satisfactory analytical and spectroscopic data, which were in full accordance with their depicted structures. Additionally, the structure of compound **E22** was further confirmed by X-ray diffraction. Its crystal data are presented in Table 1 and Fig. 4 gives a perspective view of this compound together with the atomic labeling system.

2.2. Biological activity

2.2.1. Antibacterial activity

All the synthesized vanillic acylhydrazone derivatives **E1**−**E30** were evaluated for their antimicrobial activities against two Gram-negative bacterial strains: *E. coli* ATCC 25922 and *Pseudomonas aeruginosa* ATCC 27853 and two Gram-positive bacterial strains: *Staphylococcus aureus* ATCC 6538 and *Bacillus subtilis* ATCC 530 by the standard two-fold serial broth dilution method [32,33]. The MICs (minimum inhibitory concentrations) of those compounds against these bacteria were presented in Table 2. DDCP [34] and standard antibacterial agent kanamycin B were also screened under identical conditions for comparison. The results revealed that most of the synthetic compounds exhibited significant antibacterial activities.

Out of the 30 vanillic acylhydrazone derivatives, compound **E9** displayed the most potent activity with MIC values of 0.39, 0.39,

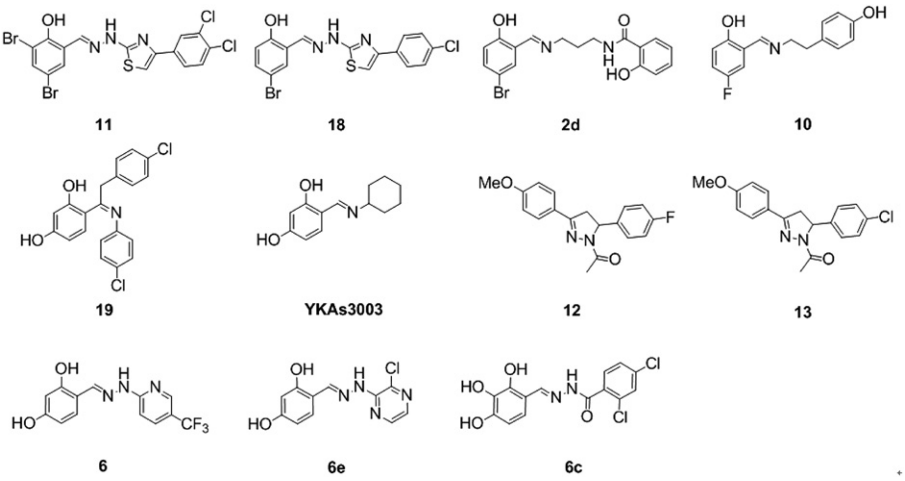

Fig. 2. New potential FabH inhibitors: **11**, **18**, **2d**, **10**, **19**, **12** and **13** discovered by Zhu et al.; **YKAs3003**, **6**, **6e** and **6c** discovered by Kim et al.

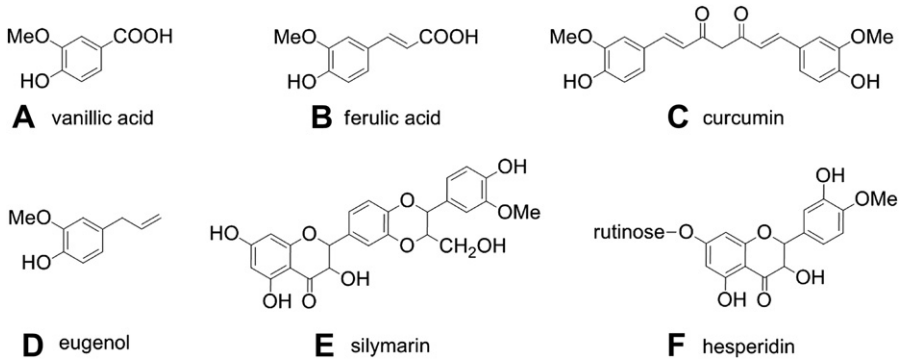

Fig. 3. Natural products **A**–**F** containing a benzene-1-methoxy-2-ol scaffold.

1.56 and 0.78 μg/mL against *E. coli*, *P. aeruginosa*, *S. aureus* and *B. subtilis* respectively, which was superior to DDCP and kanamycin B with corresponding MIC values of 3.13, 1.56, 12.5, 25 μg/mL and 0.78, 0.78, 1.56, 1.56 μg/mL, respectively.

Compounds **11**, **18**, **2d**, **10**, **19**, **12** and **13** in previous studies of our laboratory displayed broad-spectrum antimicrobial activity against all tested bacterial strains (*E. coli*, *P. aeruginosa*, *S. aureus* and *B. subtilis*) with MIC values of 0.78–25 μg/mL [13–17]. **YKAs3003** displayed MIC values in the range 128–256 μg/mL against various bacteria [18]. Besides, compounds **6** and **6c** also displayed broad-spectrum antimicrobial activity against bacterial strains (*E. coli*, *E. faecalis*, *VREF* and *S. aureus*) with MIC values of 4–64 μg/mL; But **6e** showed selective antimicrobial activity against *S. aureus* with MIC values of 1–2 μg/mL while the MIC values against other bacterial strains were 32 to >512 μg/mL [19]. Compared to the compounds in previous studies, our compound **E9** showed much more potent broad-spectrum antibacterial activity with the MIC values of 0.39–1.56 μg/mL against the tested bacterial strains. The results suggested further structural optimization leaded to a positive result in a significant increase of its antibacterial activity.

Subsequently structure–activity relationships (SAR) studies were performed to determine how the substituents on benzene ring affected the antimicrobial activity. Compound **E1** without any substituent group on benzene ring showed moderate antimicrobial activity with the mean MIC values of 25, 12.5, 25 and 25 μg/mL against *E. coli*, *P. aeruginosa*, *S. aureus* and *B. subtilis*, respectively.

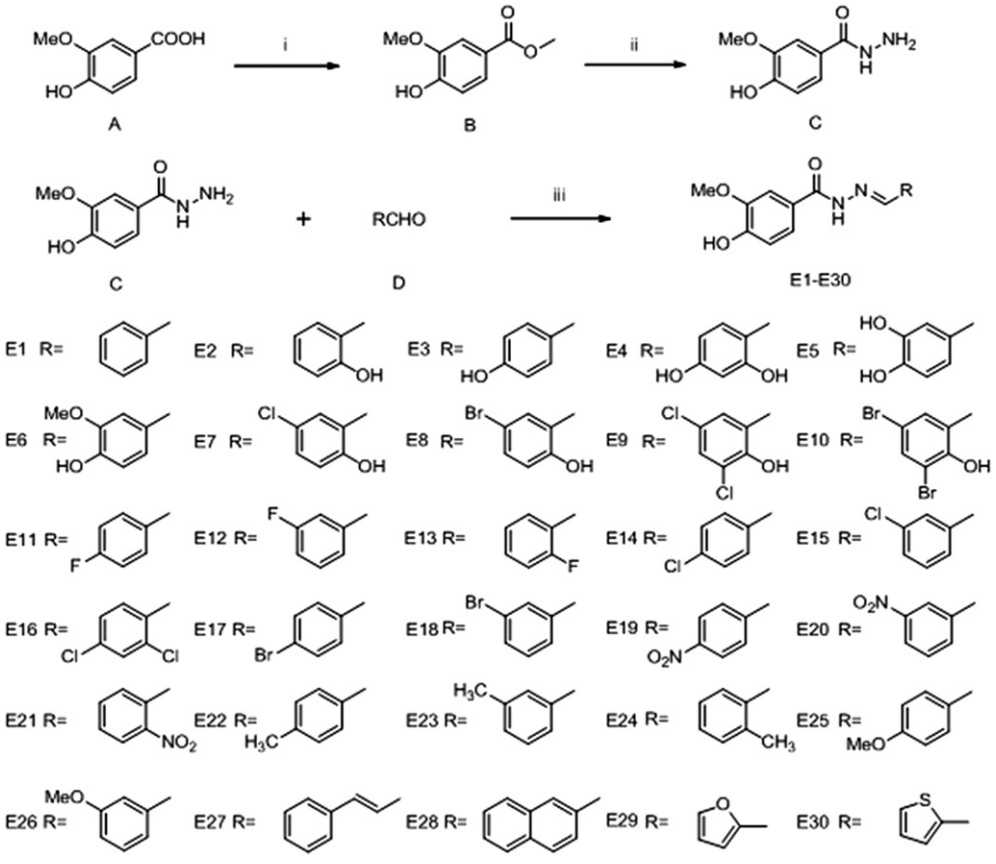

Scheme 1. General synthesis of compounds **E1**–**E30**. Reagents and conditions: (i) methanol, concentrated sulfuric acid; reflux; (ii) $NH_2NH_2 \cdot H_2O$, ethanol; 90 °C; (iii) ethanol, water, acetic acid; rt.

Table 1
Crystal data for compound **E22**.

Crystal parameters	Compound **E22**
Formula	$C_{16}H_{16}N_2O_3$
Crystal size (mm)	0.1 × 0.1 × 0.2
Formula weight	284.12
Crystal system	Monoclinic
α (°)	90.00
β (°)	99.441(7)
γ (°)	90.00
a (Å)	12.002(8)
b (Å)	8.592(6)
c (Å)	15.569(10)
V (Å^3)	1583.6(18)
Z	4
θ limits (°)	$2.34 \le h \le 26.00$
hkl limits	$-14 \le h \le 14$, $-10 \le k \le 10$, $-19 \le l \le 14$
F (000)	704
Data/restraints/parameters	3092/0/190
Absorption coefficient	0.130
Reflections collected	7637
Independent reflections	3092 [$R_{int} = 0.0499$]
R_1/wR_2 [$I > 2\&Gs(I)$]	0.2767/0.6485
R_1/wR_2 (all data)	0.3159/0.6810
GOF	3.002

Then, we evaluated the effect of introducing different substituent group(s) on benzene ring in **E1**. Firstly, introducing hydroxyl group(s) on the benzene ring in **E1** to form a class of compounds (**E2**–**E6**) increased the antimicrobial activity. **E2** with the hydroxyl group on the ortho-position of benzene ring showed MIC values of 3.13–6.25 μg/mL which was better than that of **E3** (12.5–50 μg/mL) with the hydroxyl group on the para-position of benzene ring. **E4** with two hydroxyl groups on the ortho-position and para-position of benzene ring whose MIC values (1.56–3.13 μg/mL) was superior to that of **E5** (12.5–25 μg/mL) with two hydroxyl groups on the para-position and meta-position of benzene ring. And the MIC values of **E6** with hydroxyl group on the para-position and methoxyl group on the meta-position of benzene ring was in the range of 12.5–25 μg/mL. The results indicated that the potent inhibitory activity order of compounds with hydroxyl group(s) on the benzene ring was ortho > 2,4-disubstituted > 3,4-disubstituted > para.

Secondly, compounds **E7**–**E10** condensed by a series of substituted salicylaldehyde and 4-hydroxy-3-methoxybenzohydrazide showed potent antimicrobial activities with MIC values of 0.39–25 μg/mL, especially for **E9** with two chlorine atoms on the 3-position and 5-position of salicylaldehyde whose MIC values were 0.39–1.56 μg/mL. Compound **E7** with a chlorine atom on the 5-position of salicylaldehyde displayed lower antibacterial activity than **E9** and when the substitute happened on the same position of benzene ring, the potency order was Cl > Br. For example, **E7** (3.13–6.25 μg/mL) > **E8** (12.5–25 μg/mL); **E9** (0.39–1.56 μg/mL) > **E10** (3.13–12.5 μg/mL). Besides, compared to **E2**, **E9** showed better antibacterial activities. It referred that the 4-hydrazonomethyl-benzene-2,4-dichloro-1-ol moiety is an important core structure for the antibacterial activity of **E9**.

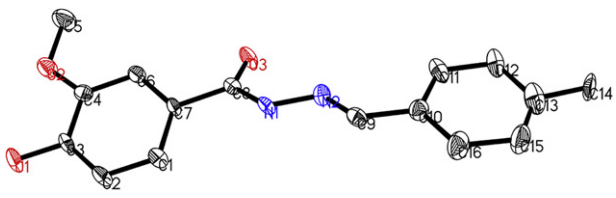

Fig. 4. Crystal structure diagram of compound **E22**.

Table 2
Antimicrobial activity of the synthesized compounds.

Compounds	Minimum inhibitory concentrations (μg/mL)			
	Gram-negative		Gram-positive	
	E. coli	*P. aeruginosa*	*S. aureus*	*B. subtilis*
E1	25	12.5	25	25
E2	1.56	1.56	3.13	3.13
E3	12.5	25	50	25
E4	3.13	6.25	6.25	6.25
E5	12.5	25	12.5	12.5
E6	25	12.5	25	12.5
E7	6.25	3.13	6.25	6.25
E8	12.5	25	12.5	25
E9	0.39	0.39	1.56	0.78
E10	6.25	3.13	12.5	6.25
E11	50	25	50	25
E12	25	12.5	25	25
E13	25	50	50	50
E14	50	25	25	50
E15	25	12.5	25	25
E16	>50	>50	>50	>50
E17	25	25	25	50
E18	50	50	25	>50
E19	25	25	50	50
E20	25	25	50	50
E21	>50	>50	>50	>50
E22	25	25	12.5	25
E23	12.5	6.25	12.5	12.5
E24	25	25	50	25
E25	50	50	>50	50
E26	25	12.5	25	25
E27	25	25	50	50
E28	25	12.5	25	25
E29	25	25	50	50
E30	50	>50	>50	>50
DDCP	3.13	1.56	12.5	25
Kanamycin B	1.56	1.56	3.13	3.13

Thirdly, the introduction of the electron-withdrawing groups (halogen groups or $-NO_2$) at the position of benzene ring weakened the antimicrobial effects. For example, compounds **E11**–**E18** with halogen group(s) and **E19**–**E21** with nitro group on benzene ring exhibited poor activities with MIC values of both 25 to >50 μg/mL. However, the introduction of the electron-donating groups (here it was $-CH_3$ or $-OCH_3$) at the position of benzene ring slightly strengthened the antimicrobial effects of compounds **E22**–**E26** with MIC values of 6.25–50 μg/mL. Among them, **E23** with a meta-methyl group on benzene ring showed the best antibacterial activity in the range of 6.25–12.5 μg/mL.

Finally, the benzene ring of **E1** was replaced with naphthalene ring, furan ring or thiophene ring respectively (**E28**–**E30**), which resulted in an obvious decrease in potency with MIC values of 25 to >50 μg/mL. This suggested that the benzene ring contributed to the antibacterial activity of our compounds.

2.2.2. *E. coli* FabH inhibitory activity

In addition, we selected the top 9 compounds (**E1**, **E2**, **E3**, **E4**, **E5**, **E7**, **E8** **E9** and **E23**) and the bottom 3 compounds (**E16**, **E21** and **E30**) of antibacterial activity according to their MIC values to examine their *E. coli* FabH inhibitory activity and the results were summarized in Table 3. As shown in Table 3, all the bottom compounds showed poor *E. coli* FabH inhibitory activities while most of the top compounds displayed potent *E. coli* FabH inhibitory activities. Among the tested compounds, **E9** showed the most potent inhibitory activity with IC_{50} of 2.5 μM, which was comparable to the positive control DDCP [34] with IC_{50} of 2.8 μM. Other tested top compounds displayed moderate inhibitory activity with IC_{50} ranging from 10.5 to 45.8 μM while the IC_{50} of the bottom 3

Table 3
E. coli FabH inhibitory activities, hemolytic activities and cytotoxicity of the selected compounds.

Compounds	*E. coli* FabH	Hemolysis	Cytotoxicity
	IC_{50} (μM)	LC30[a] (mg/mL)	IC_{50} (μM)
E1	41.2	>10	143.1
E2	13.8	>10	155.3
E3	23.2	>10	113.4
E4	11.3	>10	158.6
E5	24.1	>10	123.7
E7	12.6	>10	180.4
E8	14.7	>10	200.6
E9	2.1	>10	130.5
E16	>100	>10	125.6
E21	>100	>10	232.3
E23	28.9	>10	198.4
E30	>100	>10	210.5
DDCP	2.6	>10	123.7

[a] Lytic concentration 30%.

compounds was all >100 μM. The results indicated that **E9** had a high binding affinity with *E. coli* FabH, which supported the potent antibacterial activity of **E9**.

Then, an analysis between the antibacterial activity against *E. coli* and the *E. coli* FabH inhibitory activity of the top 9 compounds (**E1**, **E2**, **E3**, **E4**, **E5**, **E7**, **E8**, **E9** and **E23**) indicated that there was a moderate correlation between FabH inhibition and inhibition of *E. coli* cellular proliferation, as evidenced in Fig. 5, with a correlation coefficient of 1.5808, *R* square value 0.9146.

The results of *E. coli* FabH inhibitory activities of the test compounds were corresponding to the structure–activity relationships (SAR) of their antibacterial activities. This demonstrated that the potent antibacterial activities of the synthetic compounds were probably correlated to their FabH inhibitory activities.

However, *P. aeruginosa* was reported to have a different FabH with *E. coli*. So it is curious indeed that the MIC for **E9** in these two strains is the same. Fortunately, we evaluated the antibacterial activities of our compounds with both MIC and IC_{50} values (not listed) when we did the bioassay. Although MIC values are the same, the effect of anti-proliferation is different. The data indicated that the antibacterial activities of our compounds against *E. coli* were better than that of *P. aeruginosa*, including compound **E9**. The IC_{50} value of compound **E9** against *E. coli* and *P. aeruginosa* are 0.81 and 2.14 μM, respectively. This suggested that our compounds maybe acting as multi-kinase inhibitors, and FabH was one of their targets. In addition, the antibacterial effects of our compounds against *P. aeruginosa* are more likely to off-target due to inhibit targets, such as FabB, FabF and other enzymes in FAS pathway or even other pathways.

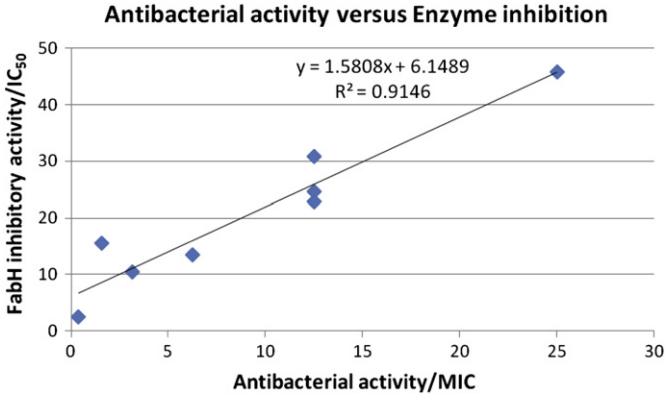

Fig. 5. Correlation between the antibacterial activity against *E. coli* and the *E. coli* FabH inhibitory activity, $r = 1.5808$, $R^2 = 0.9146$.

2.2.3. Cytotoxicity test

In order to find potent antibiotics, it is important to measure cytotoxicity. One of the major hindrances to the clinical use of many compounds with effective antibacterial activities, however, is their ability to damage mammalian cell that leads to high hemolytic and cytotoxic activity dangerous to the host organism. Hemolytic activity is conventionally used as a measure of cytotoxicity and model for mammalian cells because red blood cells are, in general, extremely fragile. However, sometimes, compounds which show low hemolytic activities have the severe cytotoxicity against mammalian cells. So the hemolysis and cytotoxicity assays were both tested.

The compounds selected above were also detected for their hemolytic activity. Then we further tested their cytotoxic activity on a mouse embryonic fibroblast cell line (NIH-3T3) using the MTT assay to prove the potency of the compounds [19].

The pharmacological results of these compounds were summarized in Table 3. It can be seen from Table 3 that the selected compounds displayed low hemolytic activities. Besides, the cytotoxicity assay determined the selectivity of our compounds for bacterial over mammalian cells. What we can see from the data is that the compounds with potent inhibitory activity were low toxic.

2.3. Binding model of *E9* and *E. coli* FabH

To gain better understanding on the potency of the compound **E9** and guide further SAR studies, the molecular docking of all the synthetic acylhydrazone derivatives and *E. coli* FabH was performed on the binding model based on the *E. coli* FabH–CoA complex structure (1HNJ pdb) [35] by using the Discovery Stutio (version 3.1).

The docking calculation of all the compounds was depicted in Table 4. As shown in Table 4, our compounds had good binding affinity to FabH and the results of EDOCKER_ENERGY almost have the same trend with the structure–activity relationships of antibacterial activities, which further confirmed the correlation between the antibacterial activities and *E. coli* FabH inhibitory activities of our compounds.

Among them, compound **E9** with the most potent inhibitory activity showed the minimum data, which suggested it was mostly easy to combine with *E. coli* FabH. The binding model of compound **E9** with 1HNJ is depicted in Fig. 6. In the binding model of **E9**, **E9** is nicely bound to the 1HNJ via four hydrogen bonds with ARG 36 (H–O···H: 1.95 Å, 144.497°), GLY 209 (H–O···H: 2.25 Å, 131.92°), MET 207 (H–O···H: 2.02 Å 144.966°) and ASN 247 (H–O···H: 1.93 Å, 160.54°), which enhance the binding affinity, resulting in the increased antimicrobial activity of this compound. The binding

Table 4
CDOCKER_ENERGY of compounds and 1HNJ.

Compounds	CDOCKER ENERGY	PSA	Compounds	CDOCKER ENERGY	PSA
	ΔGb (kcal/mol)			ΔGb (kcal/mol)	
E1	−16.13	70.9	**E16**	−9.38	70.9
E2	−18.49	91.2	**E17**	−12.87	70.9
E3	−16.26	91.2	**E18**	−11.31	70.9
E4	−18.67	111.4	**E19**	−12.89	116.7
E5	−16.31	111.4	**E20**	−15.54	116.7
E6	−16.63	100.4	**E21**	−10.78	116.7
E7	−18.65	91.2	**E22**	−15.78	70.9
E8	−18.66	91.2	**E23**	−17.02	70.9
E9	−21.33	91.2	**E24**	−16.70	70.9
E10	−18.21	91.2	**E25**	−10.73	80.16
E11	−15.28	70.9	**E26**	−16.32	80.16
E12	−12.75	70.9	**E27**	−15.58	70.9
E13	−10.35	70.9	**E28**	−16.22	70.9
E14	−13.79	70.9	**E29**	−14.26	84.1
E15	−10.68	70.9	**E30**	−10.80	70.9

model of **E9** inferred that the 4-hydrazonomethyl-benzene-2,4-dichloro-1-ol moiety made the ligand easier to conduct hydrogen bond with FabH and the introduction of benzene-1-methoxy-2-ol moiety also enhanced the binding affinity, which confirmed our structural optimization. Therefore, high binding affinities resulted in strong antimicrobial activity and the initial attempt to achieve new potential antibacterial FabH inhibitors has been verified with the expected results.

However, compound **E8** showed good binding affinity for FabH with the CDOCKER_ENERGY of −18.06 kcal/mol and IC_{50} of 14.7 against FabH. Unfortunately, it showed low antimicrobial activity against *E. coli* with MIC value of 12.5 μg/mL. Then molecular polar surface area (PSA) was also calculated in Table 4, which is a very useful parameter for prediction of drug transport properties, related to the binding affinity and the cell permeability of FabH inhibitors. PSA values in the range of 55–100 $Å^2$ increase the probability of a compound being a potent inhibitor of FabH. The results shown **E8** satisfied the PSA criteria, so the interactions between **E8** and *E. coli* FabH maybe not critical for antimicrobial activity against *E. coli*.

3. Conclusions

In conclusion, a series of vanillic acylhydrazone derivatives was designed, prepared and evaluated for their antibacterial activity against *E. coli* ATCC 25922, *P. aeruginosa* ATCC 27853, *B. subtilis* ATCC 530 and *S. aureus* ATCC 25923 in order to achieve new better potential antibacterial FabH inhibitors. Out of the 30 vanillic acylhydrazone derivatives, **E9** showed the most potent antibacterial activity with MIC values of 0.39–1.56 μg/mL against the tested bacterial strains and exhibited the most potent *E. coli* FabH inhibitory activity with IC_{50} of 2.5 μM. Preliminary structure–activity relationships and molecular modeling study provided further insight into interactions between the enzyme and its ligands. This study shows that **E9** is a novel compound that can be potent antimicrobial inhibitor of FabH and provides valuable information for the design of *E. coli* FabH inhibitors as antibacterial agents.

4. Experimental section

4.1. Materials and measurements

All chemicals (reagent grade) used were purchased from Sigma Aldrich (USA) and Sinopharm Chemical Reagent Co., Ltd (China). Melting points (uncorrected) were determined on a XT4 MP apparatus (Taike Corp., Beijing, China). ESI-MS spectra were recorded on a Mariner System 5304 Mass spectrometer, and ^1H NMR spectra were recorded on a Bruker DPX 300 model Spectrometer at 25 °C with TMS and solvent signals allotted as internal standards. Chemical shifts were reported in ppm (δ). Elemental analyses were performed on a CHN–O-Rapid instrument and were within ±0.4% of the theoretical values. TLC was run on the silica gel coated aluminum sheets (Silica Gel 60 Å GF_{254}, E. Merk, Germany) and visualized in UV light (254 nm).

4.2. General procedure for synthesis of the target compounds

To a stirred solution of hydrazide **C** (1 mmol) and compound **D** (1 mmol) in ethanol (15 mL), water (1 mL) was added followed by dropwise addition of glacial acetic acid (0.2 mL). The resulting mixture was stirred at room temperature until the target product precipitated from the solvent, which was collected using suction filtration and dried, followed by recrystallization in ethanol.

4.2.1. (E)-N′-Benzylidene-4-hydroxy-3-methoxybenzohydrazide (*E1*)

White powder, yield 89%; mp: 111–112 °C. ^1H NMR (300 MHz, DMSO-d_6): 3.85 (s, 3H), 6.86–6.88 (d, J = 8.22 Hz, 1H), 7.43–7.49 (m, 5H), 7.70–7.72 (d, J = 6.39 Hz, 2H), 8.44 (s, 1H), 9.70 (s, 1H), 11.60 (s, 1H). MS (ESI): 271.10 ($C_{15}H_{15}N_2O_3$, $[M+H]^+$). Anal. Calcd for $C_{15}H_{14}N_2O_3$: C, 66.66; H, 5.22; N, 10.36%. Found: C, 66.45; H, 5.21; N, 10.33%.

4.2.2. (E)-4-Hydroxy-N′-(2-hydroxybenzylidene)-3-methoxybenzohydrazide (*E2*)

White powder, yield 89%; mp: 221–222 °C. ^1H NMR (300 MHz, DMSO-d_6): 3.81 (s, 3H), 6.85–6.87 (d, J = 7.89 Hz, 1H), 7.00–7.03 (m, 2H), 7.41–7.44 (m, 1H), 7.47 (s, 1H), 7.53–7.56 (m, 2H), 8.33 (s, 1H), 9.64 (s, 1H), 9.84 (s, 1H), 11.39 (s, 1H). MS (ESI): 287.10 ($C_{15}H_{15}N_2O_4$, $[M+H]^+$). Anal. Calcd for $C_{15}H_{14}N_2O_4$: C, 62.93; H, 4.93; N, 9.79%. Found: C, 62.75; H, 4.95; N, 9.82%.

4.2.3. (E)-4-Hydroxy-N′-(4-hydroxybenzylidene)-3-methoxybenzohydrazide (*E3*)

White powder, yield 87%; mp: 245–246 °C. ^1H NMR (300 MHz, DMSO-d_6): 3.82 (s, 3H), 6.82–6.87 (m, 3H), 7.41–7.44 (m, 1H), 7.47 (s, 1H), 7.53–7.56 (m, 2H), 8.33 (s, 1H), 9.64 (s, 1H), 9.87 (s, 1H), 11.39 (s, 1H). MS (ESI): 287.10 ($C_{15}H_{15}N_2O_4$, $[M+H]^+$). Anal. Calcd for $C_{15}H_{14}N_2O_4$: C, 62.93; H, 4.93; N, 9.79%. Found: C, 62.80; H, 4.92; N, 9.75%.

4.2.4. (E)-N′-(2,4-Dihydroxybenzylidene)-4-hydroxy-3-methoxybenzohydrazide (*E4*)

White powder, yield 85%; mp: 255–256 °C. ^1H NMR (300 MHz, DMSO-d_6): 3.83 (s, 3H), 6.89–6.91 (m, 2H), 7.52 (s, 1H), 7.55 (s, 1H),

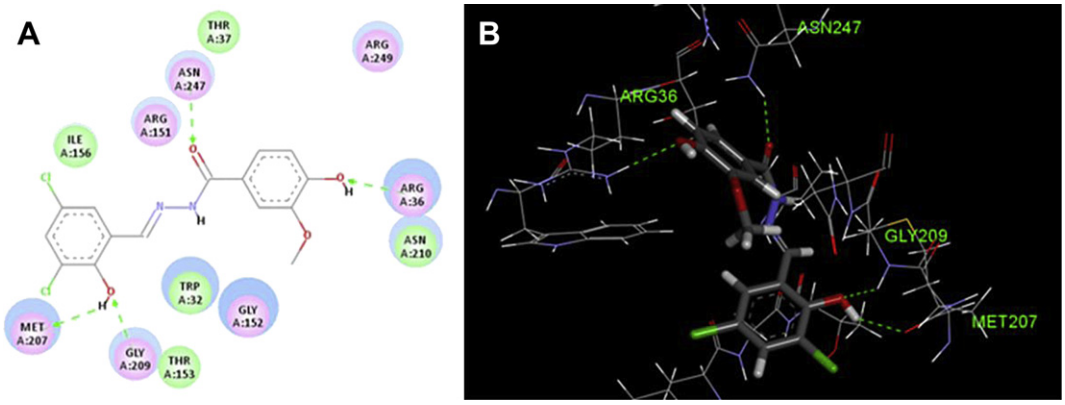

Fig. 6. (A) 2D molecular docking modeling of compound **E9** with 1HNJ. The purple circles showed the amino acids which participated in hydrogen bonding and the green circles showed the amino acids which participated in the Van der Waals interactions. (B) 3D model of the interaction between compound **E9** and 1HNJ bonding site. The four H-bonds (green lines) are displayed as dotted lines. (For interpretation of the references to colour in this figure legend, the reader is referred to the web version of this article.)

7.59–7.63 (m, 2H), 8.44 (s, 1H), 9.64 (s, 1H), 9.71 (s, 1H), 9.88 (s, 1H), 11.62 (s, 1H). MS (ESI): 303.09 ($C_{15}H_{15}N_2O_5$, $[M + H]^+$). Anal. Calcd for $C_{15}H_{14}N_2O_5$: C, 59.60; H, 4.67; N, 9.27%. Found: C, 59.80; H, 4.68; N, 9.32%.

4.2.5. (E)-N′-(3,4-Dihydroxybenzylidene)-4-hydroxy-3-methoxybenzohydrazide (**E5**)

White powder, yield 85%; mp: 260–261 °C. ^{1}H NMR (300 MHz, DMSO-d_6): 3.81 (s, 3H), 6.85 (s, 1H), 7.29–7.34 (m, 2H), 7.55 (s, 1H), 7.55–7.58 (m, 2H), 8.49 (s, 1H), 9.66 (s, 1H), 9.74 (s, 1H), 9.89 (s, 1H), 11.59 (s, 1H). MS (ESI): 303.09 ($C_{15}H_{15}N_2O_5$, $[M + H]^+$). Anal. Calcd for $C_{15}H_{14}N_2O_5$: C, 59.60; H, 4.67; N, 9.27%. Found: C, 59.77; H, 4.68; N, 9.22%.

4.2.6. (E)-4-Hydroxy-N′-(4-hydroxy-3-methoxybenzylidene)-3-methoxybenzohydrazide (**E6**)

White powder, yield 87%; mp: 102–103 °C. ^{1}H NMR (300 MHz, DMSO-d_6): 3.80 (s, 3H), 3.82 (s, 3H), 6.81–6.84 (m, 2H), 7.33–7.36 (m, 2H), 7.39–7.40 (m, 2H), 8.46 (s, 1H), 8.48 (s, 1H), 9.57 (s, 1H), 11.47 (s, 1H). MS (ESI): 317.11 ($C_{16}H_{17}N_2O_5$, $[M + H]^+$). Anal. Calcd for $C_{16}H_{16}N_2O_5$: C, 60.75; H, 5.10; N, 8.86%. Found: C, 60.58; H, 5.10; N, 8.83%.

4.2.7. (E)-N′-(5-Chloro-2-hydroxybenzylidene)-4-hydroxy-3-methoxybenzohydrazide (**E7**)

White powder, yield 92%; mp: 210–211 °C. ^{1}H NMR (300 MHz, DMSO-d_6): 3.80 (s, 3H), 6.84–6.87 (d, J = 8.43 Hz, 1H), 7.01–7.03 (m, 1H), 7.41–7.43 (m, 2H), 7.54–7.57 (m, 2H), 8.34 (s, 1H), 9.63 (s, 1H); 9.85 (s, 1H); 11.39 (s, 1H). MS (ESI): 321.06 ($C_{15}H_{14}ClN_2O_4$, $[M + H]^+$). Anal. Calcd for $C_{15}H_{13}ClN_2O_4$: C, 56.17; H, 4.09; N, 8.73%. Found: C, 56.36; H, 4.12; N, 8.77%.

4.2.8. (E)-N′-(5-Bromo-2-hydroxybenzylidene)-4-hydroxy-3-methoxybenzohydrazide (**E8**)

White powder, yield 91%; mp: 216–217 °C. ^{1}H NMR (300 MHz, DMSO-d_6): 3.81 (s, 3H), 6.87–6.88 (d, J = 7.67 Hz, 1H), 7.02–7.04 (m, 1H), 7.41–7.44 (m, 2H), 7.54–7.57 (m, 2H), 8.34 (s, 1H), 9.58 (s, 1H), 9.72 (s, 1H), 11.51 (s, 1H). MS (ESI): 365.01 ($C_{15}H_{14}BrN_2O_4$, $[M + H]^+$). Anal. Calcd for $C_{15}H_{13}BrN_2O_4$: C, 49.33; H, 3.59; N, 7.67%. Found: C, 49.10; H, 3.61; N, 7.70%.

4.2.9. (E)-N′-(3,5-Dichloro-2-hydroxybenzylidene)-4-hydroxy-3-methoxybenzohydra-zide (**E9**)

White powder, yield 90%; mp: 180–181 °C. ^{1}H NMR (300 MHz, DMSO-d_6): 3.81 (s, 3H), 6.85–6.88 (s, 1H), 7.22–7.24 (m, 1H), 7.43–7.47 (m, 1H), 7.51 (s, 1H), 7.54–7.57 (m, 1H), 8.34 (s, 1H), 9.58 (s, 1H), 9.72 (s, 1H), 11.51 (s, 1H). MS (ESI): 355.02 ($C_{15}H_{13}Cl_2N_2O_4$, $[M + H]^+$). Anal. Calcd for $C_{15}H_{12}Cl_2N_2O_4$: C, 50.72; H, 3.41; N, 7.89%. Found: C, 50.92; H, 3.42; N, 7.91%.

4.2.10. (E)-N′-(3,5-Dibromo-2-hydroxybenzylidene)-4-hydroxy-3-methoxybenzohydrazide (**E10**)

White powder, yield 84%; mp: 204–205 °C. ^{1}H NMR (300 MHz, DMSO-d_6): 3.81 (s, 3H), 6.84–6.87 (s, 1H), 7.22–7.25 (m, 1H), 7.41–7.45 (m, 1H), 7.50 (s, 1H), 7.53–7.57 (m, 1H), 8.38 (s, 1H), 9.49 (s, 1H), 9.68 (s, 1H), 11.47 (s, 1H). MS (ESI): 442.92 ($C_{15}H_{13}Br_2N_2O_4$, $[M + H]^+$). Anal. Calcd for $C_{15}H_{12}Br_2N_2O_4$: C, 40.57; H, 2.72; N, 6.31%. Found: C, 40.69; H, 2.71; N, 6.29%.

4.2.11. (E)-N′-(4-Fluorobenzylidene)-4-hydroxy-3-methoxybenzohydrazide (**E11**)

White powder, yield 89%; mp: 196–197 °C. ^{1}H NMR (300 MHz, DMSO-d_6): 3.81–3.83 (m, 3H), 6.84–6.87 (d, J = 8.35 Hz, 1H), 7.41–7.73 (m, 4H), 7.51–7.73 (d, J = 8.4 Hz, 2H), 8.41 (s, 1H), 9.69 (s, 1H), 11.65 (s, 1H). MS (ESI): 289.09 ($C_{15}H_{14}FN_2O_3$, $[M + H]^+$). Anal. Calcd for $C_{15}H_{13}FN_2O_3$: C, 62.50; H, 4.55; N, 9.72%. Found: C, 62.68; H, 4.56; N, 9.75%.

4.2.12. (E)-N′-(3-Fluorobenzylidene)-4-hydroxy-3-methoxybenzohydrazide (**E12**)

White powder, yield 92%; mp: 102–103 °C. ^{1}H NMR (300 MHz, DMSO-d_6): 3.82 (s, 3H), 6.85–6.87 (d, J = 8.43 Hz, 1H), 7.41–7.44 (m, 2H), 7.47 (s, 1H), 7.53–7.56 (m, 2H), 8.33 (s, 1H), 9.64 (s, 1H), 9.87 (s, 1H), 11.39 (s, 1H). MS (ESI): 289.09 ($C_{15}H_{14}FN_2O_3$, $[M + H]^+$). Anal. Calcd for $C_{15}H_{13}FN_2O_3$: C, 62.50; H, 4.55; N, 9.72%. Found: C, 62.70; H, 4.57; N, 9.75%.

4.2.13. (E)-N′-(2-Fluorobenzylidene)-4-hydroxy-3-methoxybenzohydrazide (**E13**)

White powder, yield 90%; mp: 114–115 °C. ^{1}H NMR (300 MHz, DMSO-d_6): 3.82 (s, 3H), 6.86–6.89 (d, J = 8.04 Hz, 1H), 7.27–7.33 (m, 2H), 7.44–7.49 (m, 3H), 7.93 (s, 1H), 8.69 (s, 1H), 9.73 (s, 1H), 11.74 (s, 1H). MS (ESI): 289.09 ($C_{15}H_{14}FN_2O_3$, $[M + H]^+$). Anal. Calcd for $C_{15}H_{13}FN_2O_3$: C, 62.50; H, 4.55; N, 9.72%. Found: C, 62.67; H, 4.57; N, 9.76%.

4.2.14. (E)-N′-(4-Chlorobenzylidene)-4-hydroxy-3-methoxybenzohydrazide (**E14**)

White powder, yield 93%; mp: 211–212 °C. ^{1}H NMR (300 MHz, DMSO-d_6): 3.85 (s, 3H), 6.84–6.89 (d, J = 6.96 Hz, 1H), 7.27–7.33 (t, J = 8.97 Hz, 2H), 7.27–7.49 (m, 2H), 7.74–7.79 (m, 2H), 8.44 (s, 1H), 9.70 (s, 1H), 11.61 (s, 1H). MS (ESI): 305.06 ($C_{15}H_{14}ClN_2O_3$, $[M + H]^+$). Anal. Calcd for $C_{15}H_{13}ClN_2O_3$: C, 59.12; H, 4.30; N, 9.19%. Found: C, 59.08; H, 4.31; N, 9.23%.

4.2.15. (E)-N′-(3-Chlorobenzylidene)-4-hydroxy-3-methoxybenzohydrazide (**E15**)

White powder, yield 89%; mp: 223–224 °C. ^{1}H NMR (300 MHz, DMSO-d_6): 3.85 (s, 3H), 6.87–6.90 (d, J = 7.68 Hz, 1H), 7.38–7.49 (m, 3H), 7.61–7.64 (m, 1H), 7.70–7.72 (m, 1H), 7.91 (s, 1H), 8.41 (s, 1H), 9.74 (s, 1H), 11.73 (s, 1H). MS (ESI): 305.06 ($C_{15}H_{14}ClN_2O_3$, $[M + H]^+$). Anal. Calcd for $C_{15}H_{13}ClN_2O_3$: C, 59.12; H, 4.30; N, 9.19%. Found: C, 58.92; H, 4.30; N, 9.22%.

4.2.16. (E)-N′-(2,4-Dichlorobenzylidene)-4-hydroxy-3-methoxybenzohydrazide (**E16**)

White powder, yield 88%; mp: 128–129 °C. ^{1}H NMR (300 MHz, DMSO-d_6): 3.85 (s, 3H), 6.86–6.89 (d, J = 8.04 Hz, 1H), 7.44–7.54 (m, 3H), 7.72–7.73 (d, J = 2.01 Hz, 1H), 8.00–8.03 (d, J = 7.86 Hz, 1H), 8.78 (s, 1H), 9.76 (s, 1H), 11.89 (s, 1H). MS (ESI): 339.02 ($C_{15}H_{13}Cl_2N_2O_3$, $[M + H]^+$). Anal. Calcd for $C_{15}H_{12}Cl_2N_2O_3$: C, 53.12; H, 3.57; N, 8.26%. Found: C, 53.01; H, 3.56; N, 8.23%.

4.2.17. (E)-N′-(4-Bromobenzylidene)-4-hydroxy-3-methoxybenzohydrazide (**E17**)

White powder, yield 90%; mp: 124–125 °C. ^{1}H NMR (300 MHz, DMSO-d_6): 3.84 (s, 3H), 6.85–6.88 (d, J = 8.04 Hz, 1H), 7.43–7.48 (m, 2H), 7.66 (s, 4H), 8.41 (s, 1H), 9.72 (s, 1H), 11.67 (s, 1H). MS (ESI): 349.01 ($C_{15}H_{14}BrN_2O_3$, $[M + H]^+$). Anal. Calcd for $C_{15}H_{13}BrN_2O_3$: C, 51.60; H, 3.75; N, 8.02%. Found: C, 51.81; H, 3.78; N, 8.06%.

4.2.18. (E)-N′-(3-Bromobenzylidene)-4-hydroxy-3-methoxybenzohydrazide (**E18**)

White powder, yield 93%; mp: 113–114 °C. ^{1}H NMR (300 MHz, DMSO-d_6): 3.85 (s, 3H), 6.86–6.89 (d, J = 8.25 Hz, 1H), 7.39–7.49 (m, 3H), 7.60–7.63 (d, J = 8.04 Hz, 1H), 7.69–7.72 (d, J = 7.5 Hz, 1H), 7.91 (s, 1H), 8.40 (s, 1H), 9.73 (s, 1H), 11.74 (s, 1H). MS (ESI): 349.0 ($C_{15}H_{14}BrN_2O_3$, $[M + H]^+$). Anal. Calcd for $C_{15}H_{13}BrN_2O_3$: C, 51.60; H, 3.75; N, 8.02%. Found: C, 51.40; H, 3.76; N, 8.05%.

*4.2.19. (E)-4-Hydroxy-3-methoxy-N′-(4-nitrobenzylidene) benzohydrazide (**E19**)*

Yellow powder, yield 93%; mp: 189–190 °C. ^{1}H NMR (300 MHz, DMSO-d_6): 3.86 (s, 3H), 6.88–6.91 (d, J = 8.25 Hz, 1H), 7.46–7.60 (m, 2H), 7.96–8.00 (d, J = 8.58 Hz, 2H), 8.29–8.32 (d, J = 8.76 Hz, 2H), 8.53 (s, 1H), 9.77 (s, 1H), 11.91 (s, 1H). MS (ESI): 316.09 ($C_{15}H_{14}N_3O_5$, $[M + H]^+$). Anal. Calcd for $C_{15}H_{13}N_3O_5$: C, 57.14; H, 4.16; N, 13.33%. Found: C, 57.01; H, 4.17; N, 13.35%.

*4.2.20. (E)-4-Hydroxy-3-methoxy-N′-(3-nitrobenzylidene) benzohydrazide (**E20**)*

Yellow powder, yield 85%; mp: 193–194 °C. ^{1}H NMR (300 MHz, DMSO-d_6): 3.84 (s, 3H), 6.88–6.90 (d, J = 8.01 Hz, 1H), 7.47–7.54 (m, 2H), 7.68–7.72 (m, 2H), 7.84–7.88 (m, 1H), 8.07–8.15 (m, 1H), 8.90 (s, 1H), 9.76 (s, 1H), 11.93 (s, 1H). MS (ESI): 316.09 ($C_{15}H_{14}N_3O_5$, $[M + H]^+$). Anal. Calcd for $C_{15}H_{13}N_3O_5$: C, 57.14; H, 4.16; N, 13.33%. Found: C, 57.29; H, 4.14; N, 13.34%.

*4.2.21. (E)-4-Hydroxy-3-methoxy-N′-(2-nitrobenzylidene) benzohydrazide (**E21**)*

Yellow powder, yield 86%; mp: 198–199 °C. ^{1}H NMR (300 MHz, DMSO-d_6): 3.85 (s, 3H), 6.87–6.90 (d, J = 8.04 Hz, 1H), 7.46–7.50 (d, J = 9.27 Hz, 2H), 7.64–7.70 (t, J = 5.12 Hz, 1H), 7.79–7.84 (t, J = 7.5 Hz, 1H), 8.05–8.13 (m, 2H), 8.88 (s, 1H), 9.75 (s, 1H), 11.95 (s, 1H). MS (ESI): 316.09 ($C_{15}H_{14}N_3O_5$, $[M + H]^+$). Anal. Calcd for $C_{15}H_{13}N_3O_5$: C, 57.14; H, 4.16; N, 13.33%. Found: C, 57.01; H, 4.17; N, 13.37%.

*4.2.22. (E)-4-Hydroxy-3-methoxy-N′-(4-methylbenzylidene) benzohydrazide (**E22**)*

White powder, yield 87%; mp: 124–125 °C. ^{1}H NMR (300 MHz, DMSO-d_6): 2.34 (s, 3H); 3.85 (s, 3H), 6.85–6.88 (d, J = 8.25 Hz, 1H), 7.25–7.27 (d, J = 7.71 Hz, 2H), 7.42–7.47 (m, 2H), 7.59–7.62 (d, J = 7.71 Hz, 2H), 8.40 (s, 1H), 9.67 (s, 1H), 11.52 (s, 1H). MS (ESI): 285.12 ($C_{16}H_{17}N_2O_3$, $[M + H]^+$). Anal. Calcd for $C_{16}H_{16}N_2O_3$: C, 67.59; H, 5.67; N, 9.85%. Found: C, 67.41 H, 5.67; N, 9.89%.

*4.2.23. (E)-4-Hydroxy-3-methoxy-N′-(3-methylbenzylidene) benzohydrazide (**E23**)*

White powder, yield 87%; mp: 135–136 °C. ^{1}H NMR (300 MHz, DMSO-d_6): 2.50 (s, 3H), 3.86 (s, 3H), 6.86–6.89 (d, J = 8.34 Hz, 1H), 7.20–7.21 (d, J = 8.01 Hz, 1H), 7.26–7.28 (d, J = 7.76 Hz, 1H), 7.42–7.47 (m, 2H), 7.59–7.63 (m, 2H), 8.48 (s, 1H), 9.69 (s, 1H), 11.54 (s, 1H). MS (ESI): 285.12 ($C_{16}H_{17}N_2O_3$, $[M + H]^+$). Anal. Calcd for $C_{16}H_{16}N_2O_3$: C, 67.59; H, 5.67; N, 9.85%. Found: C, 67.77 H, 5.66; N, 9.87%.

*4.2.24. (E)-4-Hydroxy-3-methoxy-N′-(2-methylbenzylidene) benzohydrazide (**E24**)*

White powder, yield 89%; mp: 153–154 °C. ^{1}H NMR (300 MHz, DMSO-d_6): 2.45 (s, 3H), 3.87 (s, 3H), 6.86–6.88 (d, J = 7.65 Hz, 1H), 7.23–7.25 (m, 2H), 7.40–7.46 (m, 2H), 7.57–7.60 (m, 2H), 8.46 (s, 1H), 9.68 (s, 1H), 11.51 (s, 1H). MS (ESI): 285.12 ($C_{16}H_{17}N_2O_3$, $[M + H]^+$). Anal. Calcd for $C_{16}H_{16}N_2O_3$: C, 67.59; H, 5.67; N, 9.85%. Found: C, 67.45; H, 5.66; N, 9.87%.

*4.2.25. (E)-4-Hydroxy-3-methoxy-N′-(4-methoxybenzylidene) benzohydrazide (**E25**)*

White powder, yield 85%; mp: 118–119 °C. ^{1}H NMR (300 MHz, DMSO-d_6): 3.81 (s, 3H), 3.84 (s, 3H), 6.84–6.87 (d, J = 8.25 Hz, 1H), 7.00–7.03 (m, J = 8.76 Hz, 2H), 7.41–7.47 (m, 2H), 7.64–7.67 (m, J = 6.75 Hz, 2H), 8.38 (s, 1H), 9.67 (s, 1H), 11.46 (s, 1H). MS (ESI): 301.11 ($C_{16}H_{17}N_2O_4$, $[M + H]^+$). Anal. Calcd for $C_{16}H_{16}N_2O_4$: C, 63.93; H, 5.37; N, 9.33%. Found: C, 63.80; H, 5.36; N, 9.36%.

*4.2.26. (E)-4-Hydroxy-3-methoxy-N′-(3-methoxybenzylidene) benzohydrazide (**E26**)*

White powder, yield 89%; mp: 174–175 °C. ^{1}H NMR (300 MHz, DMSO-d_6): 3.81 (s, 3H), 3.85 (s, 3H), 6.86–6.89 (d, J = 8.22 Hz, 1H), 6.99–7.02 (m, 1H), 7.26–7.28 (m, 2H), 7.35–7.40 (m, 2H), 7.48–7.49 (m, 1H), 8.42 (s, 1H), 9.71 (s, 1H), 11.62 (s, 1H). MS (ESI): 301.11 ($C_{16}H_{17}N_2O_4$, $[M + H]^+$). Anal. Calcd for $C_{16}H_{16}N_2O_4$: C, 63.99; H, 5.37; N, 9.33%. Found: C, 63.80; H, 5.35; N, 9.36%.

*4.2.27. (E)-4-Hydroxy-3-methoxy-N′-((E)-3-phenylallylidene) benzohydrazide (**E27**)*

White powder, yield 90%; mp: 222–223 °C. ^{1}H NMR (300 MHz, DMSO-d_6): 3.84 (s, 3H), 6.84–6.87 (d, J = 8.22 Hz, 1H), 7.03–7.06 (d, J = 8.40 Hz, 2H), 7.32–7.46 (m, 5H), 7.61–7.63 (d, J = 6.96 Hz, 2H), 8.20 (s, 1H), 9.69 (s, 1H), 11.50 (s, 1H). MS (ESI): 297.12 ($C_{17}H_{17}N_2O_3$, $[M + H]^+$). Anal. Calcd for $C_{17}H_{16}N_2O_3$: C, 68.91; H, 5.44; N, 9.45%. Found: C, 68.79; H, 5.43; N, 9.49%.

*4.2.28. (E)-4-Hydroxy-3-methoxy-N′-(naphthalen-2-ylmethylene) benzohydrazide (**E28**)*

White powder, yield 86%; mp: 144–145 °C. ^{1}H NMR (300 MHz, DMSO-d_6): 3.83 (s, 3H), 6.84–6.86 (m, 1H), 7.43–7.49 (m, 5H), 7.59–7.61 (d, J = 7.4 Hz, 2H), 7.70–7.72 (m, 2H), 8.44 (s, 1H), 9.70 (s, 1H), 11.60 (s, 1H). MS (ESI): 320.12 ($C_{19}H_{17}N_2O_3$, $[M + H]^+$). Anal. Calcd for $C_{19}H_{16}N_2O_3$: C, 71.24; H, 5.03; N, 8.74%. Found: C, 71.01; H, 5.04; N, 8.70%.

*4.2.29. (E)-N′-(Furan-2-ylmethylene)-4-hydroxy-3-methoxybenzohydrazide (**E29**)*

White powder, yield 89%; mp: 112–113 °C. ^{1}H NMR (300 MHz, DMSO-d_6): 4.08 (s, 3H), 6.62–6.64 (m, 1H), 6.85–6.91 (m, 2H), 7.41–7.46 (t, J = 8.05 Hz, 2H), 7.84 (s, 1H), 8.34 (s, 1H), 9.72 (s, 1H), 11.59 (s, 1H). MS (ESI): 260.08 ($C_{13}H_{13}N_2O_4$, $[M + H]^+$). Anal. Calcd for $C_{13}H_{12}N_2O_4$: C, 60.00; H, 4.65; N, 10.76%. Found: C, 60.11; H, 4.66; N, 10.80%.

*4.2.30. (E)-4-Hydroxy-3-methoxy-N′-(thiophen-2-ylmethylene) benzohydrazide (**E30**)*

White powder, yield 85%; mp: 115–116 °C. ^{1}H NMR (300 MHz, DMSO-d_6): 3.84 (s, 3H), 6.85–6.88 (d, J = 8.22 Hz, 1H), 7.13–7.15 (t, J = 4.31 Hz, 1H), 7.41–7.46 (m, 3H), 7.65–7.66 (d, J = 5.13 Hz, 1H), 8.66 (s, 1H), 9.71 (s, 1H), 11.55 (s, 1H). MS (ESI): 277.06 ($C_{13}H_{13}N_2O_3S$, $[M + H]^+$). Anal. Calcd for $C_{13}H_{12}N_2O_3S$: C, 56.51; H, 4.38; N, 10.14%. Found: C, 56.33; H, 4.37; N, 10.17%.

4.3. Crystal structure determination

Crystal structure determination of compound **E22** was carried out on a Nonius CAD4 diffractometer equipped with graphite-monochromated MoKα (λ = 0.71073 Å) radiation. The structure was solved by direct methods and refined on F^2 by full-matrix least squares methods using SHELX-97 [36]. All the non-hydrogen atoms were refined anisotropically. All the hydrogen atoms were placed in calculated positions and were assigned fixed isotropic thermal parameters at 1.2 times the equivalent isotropic U of the atoms to which they are attached and allowed to ride on their respective parent atoms. The contributions of these hydrogen atoms were included in the structure-factors calculations. The crystal data, data collection, and refinement parameter for the compound **E22** are listed in Table 1.

4.4. Antibacterial activity

The antibacterial activities of the synthetic compounds were tested against two Gram-negative bacterial strains: *E. coli* ATCC

25922 and *P. aeruginosa* ATCC 27853, two Gram-positive bacterial strains: *B. subtilis* ATCC 530 and *S. aureus* ATCC 25923, using method recommended by National Committee for Clinical Laboratory Standards (NCCLS).

In vitro activities of the compounds were tested in Nutrient broth (NB) for bacteria by the two-fold serial dilution method. Seeded broth (broth containing microbial spores) was prepared in NB from 24 h old bacterial cultures on nutrient agar (Hi-media) at 37 ± 1 °C. The bacterial suspension was adjusted with sterile saline to a concentration of 1 × 104–105 CFU. The tested compounds and reference drugs were prepared by two-fold serial dilution to obtain the required concentrations of 50, 25, 12.5, 6.25, 3.13, 1.56, 0.78 and 0.39 μg/mL. The tubes were incubated in BOD incubators at 37 ± 1 °C for bacteria. The MICs were recorded by visual observations after 24 h (for bacteria) of incubation. Kanamycin and DDCP were used as standards for bacterial. The observed MICs are presented in Table 2.

4.5. E. coli FabH purification and activity assay

Native *E. coli* FabH protein was overexpressed in *E. coli* DH10B cells using the pET30 vector and purified to homogeneity in three chromatographic steps (Q-Sepharose, MonoQ, and hydroxyapatite) at 4 °C. The selenomethionine-substituted protein was expressed in *E. coli* BL21 (DE3) cells and purified in a similar way. Harvested cells containing FabH were lysed by sonication in 20 mM Tris, pH 7.6, 5 mM imidazole, 0.5 M NaCl and centrifuged at 20,000 rpm for 30 min. The supernatant was applied to a Ni-NTA agarose column, washed, and eluted using a 5–500 mM imidazole gradient over 20 column volumes. Eluted protein was dialyzed against 20 mM Tris, pH 7.6, 1 mM DTT, and 100 mM NaCl. Purified FabHs were concentrated up to 2 mg/mL and stored at −80 °C in 20 mM Tris, pH 7.6, 100 mM NaCl, 1 mM DTT, and 20% glycerol for enzymatic assay.

In a final 20 μL reaction, 20 mM Na_2HPO_4, pH 7.0, 0.5 mM DTT, 0.25 mMMgCl_2, and 2.5 μM holo-ACP were mixed with 1 nM FabH, and H_2O was added to 15 μL. After 1 min incubation, a 2 μL mixture of 25 μM acetyl-CoA, 0.5 mM NADH, and 0.5 mM NADPH was added for FabH reaction for 25 min. The reaction was stopped by adding 20 μL of ice-cold 50% TCA, incubating for 5 min on ice, and centrifuging to pellet the protein. The pellet was washed with 10% ice-cold TCA and resuspended with 5 μL of 0.5 M NaOH. The incorporation of the ^3H signal in the final product was read by liquid scintillation. When determining the inhibition constant (IC_{50}), inhibitors were added from a concentrated DMSO stock such that the final concentration of DMSO did not exceed 2%.

4.6. Hemolysis test

Hemolytic activity was assayed using fresh capillary human blood. Erythrocytes were collected by centrifuging the blood three times in chilled phosphate buffered saline (PBS at 4 °C) at 1000× *g* for 10 min. The final pellet was resuspended in PBS to give a 2% w/v solution. Using a microtitre plate, 100 μL of the erythrocyte solution was added to dextran, PLL, stearyl-PLL or stearyl-PLL + LDL (1–1000/μg/mL) in a volume of 100 mL. Samples were then incubated for 3 h and the microtitre plate was centrifuged then at 1000× *g* for 10 min and the supernatants (100 μL) transferred into a new microtitre plate. Hemoglobin release was determined spectrophotometrically using a microtitre plate reader (absorbance at 550 nm). Results were expressed as the amount of released hemoglobin induced by the compounds as a percentage of the total.

4.7. Cytotoxicity test

The cytotoxic activity in vitro was measured against mouse fibroblast NIH-3T3 cells using the MTT assay. Cells were cultured in a 96-well plate at a density of 5 × 10^5 cells and different concentrations of compounds were respectively added to each well. The incubation was permitted at 37 °C, 5% CO_2 atmosphere for 24 h before the cytotoxicity assessments. 20 μL MTT reagent (4 mg/mL) was added per well 4 h before the end of the incubation. Four hours later, the plate was centrifugated at 1200 rcf for 5 min and the supernatants were removed, each well was added with 200 μL DMSO. The absorbance was measured at a wavelength of 570 nm (OD570 nm) on an ELISA microplate reader. Three replicate wells were used for each concentration and each assay was measured three times, after which the average of IC_{50} was calculated. The cytotoxicity of each compound was expressed as the concentration of compound that reduced cell viability to 50% (IC_{50}). The results were summarized in Table 3.

4.8. Docking simulations

Molecular docking of compounds **E9** into the three-dimensional X-ray structure of *E. coli* FabH (PDB code: 1HNJ) was carried out using the Discovery Stutio (version 3.1) as implemented through the graphical user interface DS-CDocker protocol.

The three-dimensional structures of the aforementioned compounds were constructed using Chem 3D ultra 12.0 software [Chemical Structure Drawing Standard; Cambridge Soft corporation, USA (2010)], then they were energetically minimized by using MMFF94 with 5000 iterations and minimum RMS gradient of 0.10. The crystal structures of *E. coli* FabH were retrieved from the RCSB Protein Data Bank (http://www.rcsb.org/pdb/home/home.-do). All bound water and ligands were eliminated from the protein and the polar hydrogen was added. The whole *E. coli* FabH was defined as a receptor and the site sphere was selected based on the ligand binding location of malonyl-CoA, then the malonyl-CoA molecule was removed and **E9** was placed during the molecular docking procedure. Types of interactions of the docked protein with ligand were analyzed after the end of molecular docking.

Acknowledgment

The work was financed by Natural Science Foundation of China (No. J1103512).

References

[1] J. Wang, et al., Nature 441 (2006) 358–361.
[2] M. Leeb, Nature 431 (2004) 892–893.
[3] J. Wang, Nat. Acad. Sci. 104 (2007) 7612–7616.
[4] R.J. Heath, C.O. Rock, Curr. Opin. Investig. Drugs 5 (2004) 146–153.
[5] S. Smith, A. Witkowski, A.K. Joshi, Prog. Lipid. Res. 42 (2003) 289–317.
[6] Z.-L. Li, Q.-S. Li, H.-J. Zhang, Y. Hu, D.-D. Zhu, H.-L. Zhu, Bioorg. Med. Chem. 19 (2011) 4413–4420.
[7] Z. Nie, C. Perretta, J. Lu, Y. Su, S. Margosiak, K.S. Gajiwala, J. Cortez, V. Nikulin, K.M. Yager, K. Appelt, S. Chu, J. Med. Chem. 48 (2005) 1596–1609.
[8] C.E. Christensen, B.B. Kragelund, P. von Wettstein-Knowles, A. Henriksen, Protein Sci. 16 (2007) 261–272.
[9] W. Bylka, I. Matlawska, N.A. Pilewski, JANA 7 (2004) 24–31.
[10] P.-J. Lee, J.B. Bhonsle, H.W. Gaona, D.P. Huddler, T.N. Heady, M. Kreishman-Deitrick, A. Bhattacharjee, W.F. McCalmont, L. Gerena, M. Lopez-Sanchez, N.E. Roncal, T.H. Hudson, J.D. Johnson, S.T. Prigge, N.C. Waters, J. Med. Chem. 52 (2009) 952–963.
[11] S. Singh, L.K. Soni, M.K. Gupta, Y.S. Prabhakar, S.G. Kaskhedikar, Eur. J. Med. Chem. 43 (2008) 1071–1080.
[12] A. Asheka, S.J. Cho, Bioorg. Med. Chem. 14 (2006) 1474–1482.
[13] P.-C. Lv, K.-R. Wang, Y. Yang, W.-J. Mao, J. Chen, J. Xiong, H.-L. Zhu, Bioorg. Med. Chem. Lett. 19 (2009) 6750–6754.
[14] H.-Q. Li, Y. Luo, P.-C. Lv, L. Shi, C.-H. Liu, H.-L. Zhu, Bioorg. Med. Chem. Lett. 20 (2010) 2025–2028.

[15] L. Shi, R.-Q. Fang, Z.-W. Zhu, Y. Yang, K. Cheng, W.-Q. Zhong, H.-L. Zhu, Eur. J. Med. Chem. 45 (2010) 4358–4364.
[16] K. Cheng, Q.-Z. Zheng, Y. Qian, L. Shi, J. Zhao, H.-L. Zhu, Bioorg. Med. Chem. 17 (2009) 7861–7871.
[17] P.-C. Lv, J. Sun, Y. Luo, Y. Yang, H.-L. Zhu, Bioorg. Med. Chem. Lett. 20 (2010) 4657–4660.
[18] J.-Y. Lee, K.-W. Jeong, J.-U. Lee, D.-I. Kang, Y. Kim, Bioorg. Med. Chem. 17 (2009) 1506–1513.
[19] J.-Y. Lee, K.-W. Jeong, S. Shin, J.-U. Lee, Y. Kim, Eur. J. Med. Chem. 47 (2012) 261–269.
[20] A.J.M. Rasras, et al., Eur. J. Med. Chem. 45 (2010) 2307–2313.
[21] A.M. Kamel, M.A. Lobna, M.L. El-Sayed, I.H. Mohamed, H.B. Rania, Bioorg. Med. Chem. 14 (2006) 8675–8682.
[22] A. Ivanova, D. Ivajla, T. Iva, K. Atanas, K. Ivanka, Zeitschrift für Naturforschung 57 (2002) 624–628.
[23] S. Wang, Z. Gao, X.-M. Chen, X.-J. Lian, H.-S. Zhu, J. Zheng, L.-Z. Sun, Biomed. Mater. 3 (2008) 1–5.
[24] P. Manikandan, M. Sumitra, S. Aishwarya, B.M. Manohar, B. Lokanadam, R.Puvanakrishnan, Int. J. Biochem. Cell. Biol. 36 (10) 1967–1980.
[25] B.B. Aggarwal, K.B. Harikumar, Int. J. Biochem. Cell. Biol. 41 (2009) 40–59.
[26] J.S. Jurenka, Altern. Med. Rev. 14 (2009) 141–153.
[27] M.-K. Kim, J.-C. Park, Y. Chong, Nat. Prod. Commun. 7 (2012) 57–58.
[28] B.B. Aggarwal, A. Kumar, A.C. Bharti, Anticancer Res. 23 (2003) 363–398.
[29] K.P. Devi, S.A. Nisha, R. Sakthivel, S.K. Pandian, J. Ethnopharmacol. 130 (2010) 107–115.
[30] T.S. Mohamed Saleem, C.M. Chetty, S. Ramkanth, V.S.T. Rajan, K.M. Kumar, K. Gauthaman, Int. J. Res. Pharm. Sci. 1 (2010) 1–5.
[31] Y. Hu, X. Lu, K. Chen, R. Yan, Q.-S. Li, H.-L. Zhu, Bioorg. Med. Chem. 20 (2012) 903–909.
[32] J.D. MacLowry, M.J. Jaqua, S.T. Selepak, Appl. Microbiol. 20 (1970) 46–53.
[33] F. Smaill, J. Can. Gastroenterol. 14 (2000) 871–875.
[34] X. He, M.R. Anne, R.D. Umesh, E.K. Glen, A.R. Kevin, Antimicrob. Agents Chemother. 48 (2004) 3093–3102.
[35] X. Qiu, C.A. Janson, W.W. Smith, M. Head, J. Lonsdale, A.K. Konstantinidis, J. Mol. Biol. 307 (2001) 341–356.
[36] R. Huey, G.M. Morris, A.J. Olson, D.S. Goodsell, J. Comput. Chem. 28 (2007) 1145–1152.